

VALIDATION OF MYOCARDIAL ELASTOGRAPHY USING MR TAGGING IN NORMAL AND ABNORMAL HUMAN HEARTS IN VIVO

Wei-Ning Lee¹, Zhen Qian², Christina L. Tosti¹, Srirama V. Swaminathan^{3,4},
Truman R. Brown^{1,4}, Dimitris N. Metaxas² and Elisa E. Konofagou^{1,4}

¹Department of Biomedical Engineering, Columbia University, New York, NY, USA, ²Department of Biomedical Engineering, Rutgers University, Piscataway, NJ, USA, ³Philips Medical Systems, Cleveland, OH, USA,

⁴Department of Radiology, Columbia University, New York, NY, USA

ABSTRACT

In this paper, Myocardial Elastography (ME), a radio-frequency (RF) based speckle tracking technique, was employed in order to assess the contractility of a myocardium, and validated against tagged Magnetic Resonance Imaging (tMRI) *in vivo* in normal as well as abnormal cases. Both RF ultrasound and tMRI frames were acquired in 2D short-axis (SA) views from two healthy subjects and one with a history of infarction. In-plane (lateral and axial) incremental displacements were iteratively estimated using 1D cross-correlation and recorrelation techniques in a 2D search with a 1D matching kernel. The incremental displacements from end-diastole (ED) to end-systole (ES) were then accumulated to obtain cumulative systolic displacements. In tMRI, cardiac motion was obtained by a template-matching algorithm on a 2D grid-shaped mesh. The entire displacement distribution within the myocardium was obtained by a cubic B-spline-based method. In both ME and tMRI, 2D Lagrangian finite systolic strains were calculated from cumulative 2D displacements. Radial and circumferential strains were then computed from the 2D finite strains. Both qualitatively and quantitatively, ME is shown capable of measuring myocardial deformation in excellent agreement with tMRI estimates in normal and abnormal subjects.

Index Terms— cross-correlation, echocardiography, elastography, MRI, myocardial, radio-frequency, strain, tagging

1. INTRODUCTION

Widely used in the clinic, echocardiography has important advantages over alternative imaging techniques owing to its higher temporal resolution, low cost, portability and familiarity to cardiologists. Myocardial Elastography (ME), which is a radio-frequency (RF) based speckle tracking technique, has shown capable of assessing normal myocardial deformation [1] and detecting abnormal myocardial function [2], due to ischemia or infarction, through estimation and imaging of the myocardial deformation during the natural contraction of the myocardium at each heart beat. We have previously

proposed a theoretical framework to analyze ME [3, 4]. This shows the excellent performance of ME in accurately depicting in-plane deformation using both a two-dimensional (2D) ultrasonic image formation model and an established three-dimensional (3D) finite-element canine left-ventricular model, in both normal and left-circumflex (LCx) ischemic cases. Not only was ME shown to accurately estimate the myocardial displacements and strains using that theoretical model, but it could also differentiate abnormal from normal cardiac muscle without a beam-to-muscle angle dependence [3].

In clinical applications, the assessment of myocardial deformation using Cardiac tagged Magnetic Resonance Imaging (tMRI) [5] is currently considered as the noninvasive gold standard. Several studies have compared the estimates from echocardiography with those from tMRI [6, 7]. Notomi et al. [6] and Helle-Valle et al. [7] have demonstrated that left-ventricular torsion measured from B-mode-based speckle tracking methods is consistent with that from tMRI in short-axis (SA) views. In this paper, we focus on the full depiction of 2D myocardial deformation, including displacements and strains, from the RF-based, and therefore more precise, ME technique, which is applied in a clinical setting in order to evaluate the myocardial motion and strain estimates and validate them against the tMRI findings.

2. METHODS

2.1 Ultrasound and MRI data acquisition

A clinical echocardiography ultrasound scanner (GE Vivid FiVe, GE Vingmed Ultrasound, Horten, Norway) with a phased array probe (FPA 2.5MHz 1C) was used to acquire cardiac ultrasound in-phase and quadrature (I/Q) data in 2D SA views at the medial left-ventricular level from two healthy and one abnormal subject at a frame rate of 136 fps. The I/Q data were upsampled to retrieve the RF signals. Tagged MR images were obtained on Philips Intera 1.5T scanner (Philips Medical Systems, Best, The Netherlands) equipped with a five-channel SENSE cardiac coil and Master gradients of strength 30 mT/m and slew rate 150 T/m/s. A Multi-slice and multi-phase true SA tagged

image was acquired under free-breathing with a combination of fast-field echo excitation and a multi-shot echo-planar readout (EPI-FFE) technique [8] (FOV=350 mm, TE=4 ms, TR=30, NSA=4, resolution acquired/reconstructed =192/256, flip angle =13 degrees, EPI factor=3 and full ECG gating scan duration=2.96 min). Two-dimensional grid tagging was performed yielding a 9-mm, in-plane tag resolution. The SA orientation was also acquired at the medial left-ventricular plane.

2.2 Myocardial Elastography (ME)

The two in-plane orthogonal displacement components (lateral and axial) were estimated using one-dimensional (1D) cross-correlation and recorrelation of RF signals in a 2D search [4]. The cross-correlation technique employed a 1D matching kernel of 7.7 mm and 80% overlap. The reference and comparison frames respectively contained the RF signals before and after deformation. An 8:1 linear interpolation scheme between two adjacent original RF signal segments of the comparison frame within the 1D kernel was employed to improve the lateral resolution [4]. The maximal cross-correlated value yielded from the RF signal segment in the comparison frame was considered the best match with the RF signal segment in the reference frame. Cosine interpolation was then applied around this maximum of the cross-correlation function for a more refined peak search.

The correction (or, recorrelation) in axial displacement estimation [4], was performed to reduce the decorrelation resulting from axial motion. In ME, recorrelation was implemented by shifting RF signal segments according to the estimated axial displacement in the comparison frame, prior to the second lateral displacement estimation.

The incremental displacements were integrated to obtain the *cumulative* displacement that occurred from ED to ES. Appropriate registration for each pixel on two consecutive displacement images was performed in order to further ensure that the cumulative displacement depicted the motion of the same tissue region.

2.3 MRI tagging (tMRI)

Tagged MRI generates two perpendicular sets of equally spaced parallel tagging plains within the myocardium as temporary markers at end-diastole through spatial modulation of the magnetization. Imaging planes were perpendicular to the two sets of tagging planes so that the tags appear as dark grids on the MR images and deform with the underlying myocardium during the cardiac cycle *in vivo*. This yielded detailed motion information of the myocardium.

In order to track the tagging grids and get the localized myocardial displacement and strain values, we implemented a template-based tracking algorithm on a 2D grid-shaped mesh to obtain the displacement vectors of the crossing points (or, nodes) on the tagging grids [9-12]. Each crossing point (or, node) on the mesh was tracked by calculating the

similarity between templates, which were modeled using two tunable Gabor filters and the underlying images. The crossing points on the mesh were driven iteratively by forces from the neighboring image patches, whose texture patterns were the most similar to a reference template. The coordinates of the crossing points in a time sequence were further smoothed by a cubic spline function, and the displacements were thus calculated through subtraction. Finally, a cubic B-spline-based method was employed to obtain the entire displacement distribution within the myocardium [13].

2.4 Strain estimation

2.4.1 Two-dimensional in-plane strains

Strain is defined in terms of the gradient of the displacement. A displacement vector, $\underline{\mathbf{u}}$, is written as $\underline{\mathbf{u}} = u_x \underline{\mathbf{e}}_x + u_y \underline{\mathbf{e}}_y$, where u_x and u_y are lateral and axial displacement components, respectively, and $\underline{\mathbf{e}}_x$ and $\underline{\mathbf{e}}_y$ are the unit vectors in the lateral and axial directions, respectively. The displacement gradient tensor \mathbf{G} in Cartesian coordinates (x, y) is thus defined as

$$\mathbf{G} = \nabla \underline{\mathbf{u}} = \begin{bmatrix} \frac{\partial u_x}{\partial x} & \frac{\partial u_x}{\partial y} \\ \frac{\partial u_y}{\partial x} & \frac{\partial u_y}{\partial y} \end{bmatrix} \quad (1)$$

The in-plane Lagrangian finite strain tensor, \mathbf{E} , is formulated as [14]

$$\mathbf{E} = \frac{1}{2}(\mathbf{G} + \mathbf{G}^T + \mathbf{G}^T \mathbf{G}) \quad (2)$$

Lateral and axial strains are the diagonal components of \mathbf{E} , i.e., \mathbf{E}_{xx} and \mathbf{E}_{yy} , respectively. In ME, a least-squares strain estimator (LSQSE) [15] with a kernel of 13.4 mm in both the lateral and axial directions was used in order to improve the signal-to-noise ratio (SNR) in the strain image (i.e., elastogram) and simultaneously have similar image resolutions between tMRI and ME in order to better facilitate subsequent comparison.

2.4.2 Radial and Circumferential Strains

The abovementioned 2D (or, lateral and axial) Lagrangian finite strains are dependent on the orientation of the ultrasound transducer relative to the ventricle. This angle-dependence may complicate the interpretation of the myocardial deformation in the left ventricle. Therefore, radial and circumferential strains are obtained by defining an angle, θ , about the centroid of the left ventricle and by transforming the finite strain tensor \mathbf{E} into a radial-circumferential strain tensor ($\hat{\mathbf{E}}$) with a transformation matrix \mathbf{Q} [14].

$$\hat{\mathbf{E}} = \mathbf{Q} \mathbf{E} \mathbf{Q}^T \quad \text{where} \quad \mathbf{Q} = \begin{bmatrix} \cos \theta & \sin \theta \\ -\sin \theta & \cos \theta \end{bmatrix} \quad (3)$$

Positive and negative radial strains indicate myocardial thickening and thinning, respectively, while myocardial stretching and shortening are represented by positive and negative circumferential strains, respectively.

3. RESULTS

The cumulative lateral, axial and radial displacement images from ED to ES estimated from tMRI and ME on a SA view of a normal left ventricle are shown in Fig. 1 (displayed on a scale of ± 7 mm at the end systolic phase).

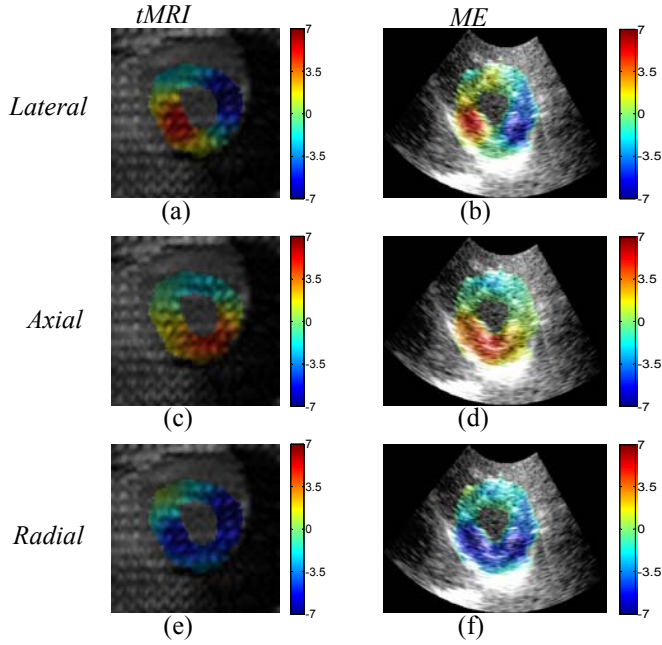


Figure 1: Normal subject: (a), (c) and (e) are the cumulative lateral, axial and radial displacements from tMRI between ED and ES, respectively; (b), (d) and (f) are the cumulative lateral, axial and radial displacements from ME between ED and ES, respectively. All the images are displayed on a scale of ± 7 mm, acquired approximately at the medial left-ventricular level and shown at ES.

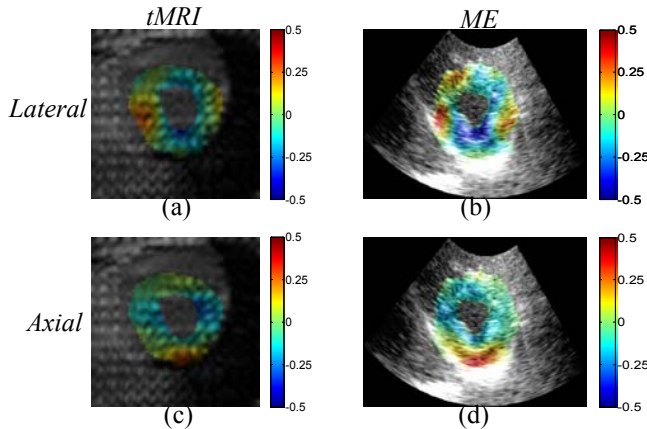


Figure 2: Normal subject: (a) and (c) are the cumulative lateral and axial systolic strains from tMRI between ED and ES, respectively; (b) and (d) are the cumulative lateral and axial systolic strains from ME between ED and ES, respectively. Strains are displayed on a scale of ± 0.5 (i.e., 50%).

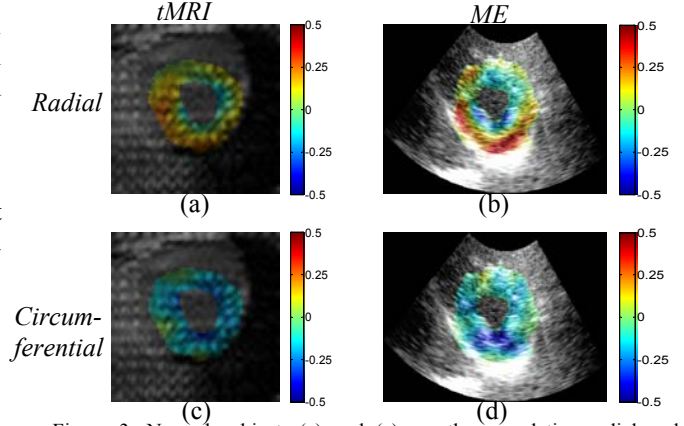


Figure 3: Normal subject: (a) and (c) are the cumulative radial and circumferential systolic strains from tMRI between ED and ES, respectively; (b) and (d) are the cumulative radial and circumferential systolic strains from ME, respectively. Strains are displayed on a scale of ± 0.5 (i.e., 50%).

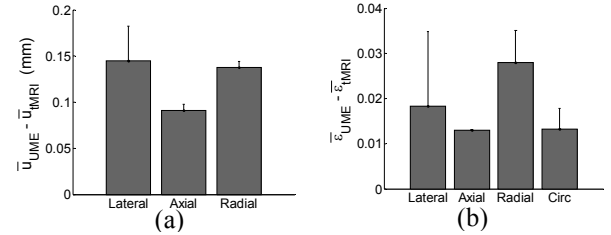


Figure 4: Normal subject: Variation of the ME-tMRI difference in the case of (a) lateral, axial and radial displacements; (b) lateral, axial, radial and circumferential strains between ME and tMRI over two healthy volunteers. \bar{u}_{UME} and \bar{u}_{tMRI} are the mean displacements in a region of 7.5-by-7.5 mm², respectively. $\bar{\epsilon}_{UME}$ and $\bar{\epsilon}_{tMRI}$ are the mean strain values in the same region in the posterior wall for ME and tMRI, respectively.

The cumulative in-plane (2D, radial and circumferential) systolic strains estimated from tMRI and ME are shown in Figs. 2 and 3 (displayed on a scale of ± 0.5 , i.e., $\pm 50\%$, at ES). The anterior, lateral, posterior and septal walls are in the upper right, lower right, lower left and upper left regions, respectively. In 2D strains (Fig. 2), positive and negative strains indicate tension and compression, respectively. Figure 3 shows positive radial (myocardial thickening) and negative circumferential (myocardial shortening) strains. The mean and standard deviation of the estimation difference of the average displacements and strains over the two normal subjects are shown in Fig. 4. The difference between ME and tMRI displacement estimates is calculated as $\bar{u}_{UME} - \bar{u}_{tMRI}$, where \bar{u}_{UME} and \bar{u}_{tMRI} are the mean strain values in a region of 7.5-by-7.5 mm² in the posterior wall for ME and tMRI, respectively. Figure 4(a) shows that the difference between ME and tMRI displacement estimates is below 0.2 mm with the displacement values ranging from -7 to 7 mm (Fig. 1). The difference between ME and tMRI strain estimates is calculated as $\bar{\epsilon}_{UME} - \bar{\epsilon}_{tMRI}$, where $\bar{\epsilon}_{UME}$ and $\bar{\epsilon}_{tMRI}$ are the mean strain values across the entire SA view. Figure 4 (b) shows that the difference of strain estimates is below 0.04 (i.e., 4% strain) with the strain values ranging from -0.5 to 0.5 (Figs.

2 and 3). The displacements and strains obtained from ME are overestimated compared with those from tMRI.

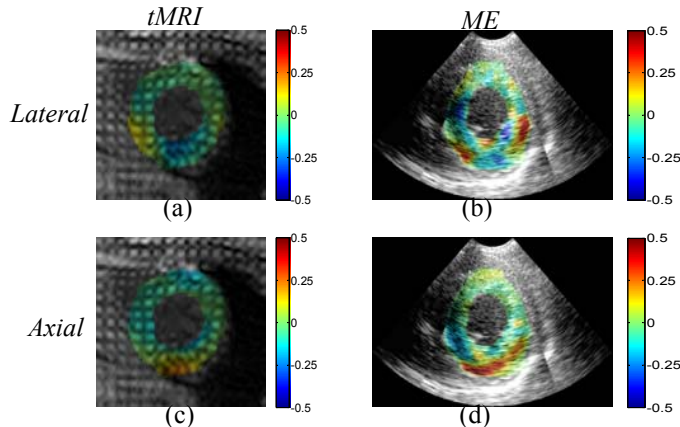


Figure 5: LAD subject: (a) and (c) are the cumulative lateral and axial systolic strains from tMRI between ED and ES, respectively; (b) and (d) are the cumulative lateral and axial systolic strains from ME between ED and ES, respectively.

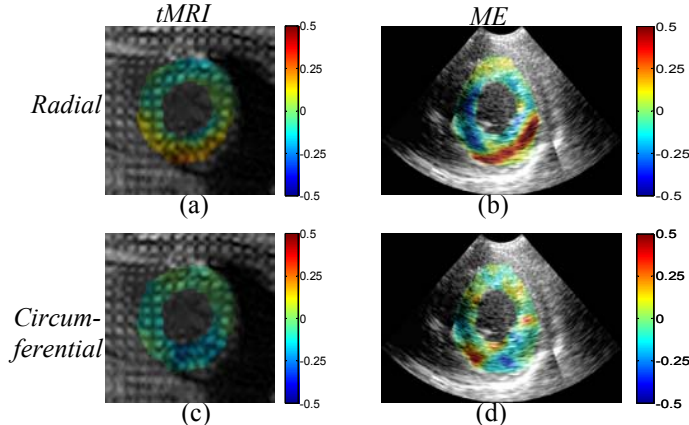


Figure 6: LAD subject: (a) and (c) are the cumulative radial and circumferential systolic strains from tMRI between ED and ES, respectively; (b) and (d) are the cumulative radial and circumferential systolic strains estimated from ME between ED and ES, respectively.

Figure 5 shows lateral and axial systolic strains estimated from tMRI and ME for a subject who had suffered from myocardial infarction caused by the occlusion of the distal LAD coronary artery and had motion abnormalities in both the septal and anterior walls. The anterior, lateral, posterior and septal walls are in the upper right, lower right, lower left and upper left regions, respectively. Not only is the magnitude of the strains of the patient smaller than those of the healthy subject (Fig. 2), but the strain pattern of the abnormal subject is not symmetric compared with the healthy subject (Fig. 2). The radial strain (Figs. 6(a) and (b)) of the patient shows myocardial thickening in the posterior and anterior-septal walls, not in part of the septum and anterior regions. Circumferential strain estimate (Fig. 6(d)) from ME shows myocardial shortening in the posterior wall and slight stretching in the other regions. Although the strains obtained from ME are overestimated compared with those from tMRI, the preliminary results show that the two

imaging modalities have good agreement and that ME is capable of differentiating abnormal from normal myocardium even in a post-infarction, treated subject.

4. DISCUSSION AND CONCLUSION

ME was able to accurately assess myocardial motion and deformation with values highly comparable to those obtained with tMRI. Axial estimates depicted the strongest agreements between the two modalities in both normal and abnormal cases. However, slight overestimation (within 8%) of the strains in normal subjects with ME compared to that with tMRI was observed, possibly resulting from the fact that the ultrasound signals suffered from low SNR, the ultrasound and tagged MR images were not acquired at exactly the same SA slice, few tagging lines were involved in the myocardium and that the spatial resolution of the strain estimates in ultrasound was higher due to the lack of tags. Future work will focus on the more accurate registration of ultrasound and tagged MR images, assessment of the role of the sonographic SNR on the ME strain estimates and study of the tradeoff between spatial resolution and strain accuracy for precise quantification in both normal and acute infarction patients.

ACKNOWLEDGEMENT

This study was supported in part by the American Heart Association (SDG 0435444T) and NIH (R01EB006042-01). The authors would like to thank Hamed Mojahed for acquiring the tagged MR images, Kana Fujikura and Donna Macmillan-Marotti for acquiring echocardiography, Simon D. Fung-Kee-Fung for developing the data acquisition protocol in ultrasound and Jianwen Luo for helpful discussion.

REFERENCES

- [1] E. E. Konofagou et al., *Ultrasound in Med. & Biol.*, vol. 28(4), pp. 475-482, 2002.
- [2] E. E. Konofagou et al., *IEEE-UFFC Symp. Proc.*, pp. 1589-1592, 2001.
- [3] S. D. Fung-Kee-Fung et al., *IEEE-UFFC Symp. Proc.*, pp. 516-519, 2005.
- [4] W.-N. Lee and E. E. Konofagou, *IEEE-UFFC Symp. Proc.*, pp. 1217-1220, 2006.
- [5] J. Declercq et al., *Phys. Med. Biol.*, vol. 45, pp. 1611-1632, 2000.
- [6] Y. Notomi et al., *J. Am. Coll. Cardiol.*, vol. 45, pp. 2034-2041, 2005.
- [7] T. Helle-Valle et al., *Circulation*, vol. 112, pp. 3149-3156, 2005.
- [8] M. Stuber et al., *Magn Reson. Med.*, vol. 41, pp. 639-643, 1999.
- [9] Z. Qian et al., *Proc. of CVIBA Workshop*, In Conjunction with ICCV, LNCS 3765, pp. 93-102, 2005.
- [10] Z. Qian, et al., *Proc. of MICCAI*, LNCS 4190, pp. 636-644, 2006.
- [11] J. Park et al., *Int. J. Med. Inform.*, vol. 55, pp. 117-126, 1999.
- [12] I. Haber et al., *Comput. Sci. Eng.*, vol. 2, pp. 18-30, 2000.
- [13] D. T. Sandwell, *Geophys. Res. Lett.*, vol. 14, pp. 139-142, 1987.
- [14] W. M. Lai et al., *Introduction to Continuum Mechanics*, 3rd ed. Butterworth-Heinemann, 1993, Chapter 2, pp. 28-32.
- [15] F. Kallel and J. Ophir, *Ultrason. Imaging*, vol. 19, pp. 195-208, 1997.